Sensitivity of Mixed Layer Predictions at Ocean Station Papa to Atmospheric Forcing Parameters

DAVID ADAMEC AND RUSSELL L. ELSBERRY

Department of Meteorology, Naval Postgraduate School, Monterey, CA 93943

(Manuscript received 1 July 1983, in final form 27 January 1984)

ABSTRACT

The effect of errors and biases in the atmospheric forcing for oceanic mixed layer model predictions is studied using data sensitivity techniques. First, the bulk model of Garwood is used to predict 17 years of mixed layer evolution and temperature structure at Ocean Station Papa using forcing derived from the 3 h atmospheric observations. The model is then integrated again varying, one at a time, each atmospheric forcing variable by a Gaussian error whose spread is proportional to the standard deviations of that variable during late winter or midsummer. The results of those integrations are then compared with the control run to assess the effects of the added random errors or biases. A positive or negative bias in the atmospheric forcing is much more detrimental to the ocean prediction than is a random error with zero mean. The predicted mixed layer depths are more sensitive to errors introduced in the forcing in winter than in summer. Conversely, the mixed layer temperature is more sensitive to errors in summer than in winter. For both winter and summer, the wind speed is the most critical factor in predicting mixed layer depth and temperature. Dew point temperature is an important variable for mixed layer predictions during the winter. During summer, cloud cover becomes an important variable. The results of this study are compared with errors in mixed layer depth and temperature predictions that are due to errors in the initial profile. The errors in the predictions which are due to errors in the atmospheric forcing are comparable in magnitude to those errors which are due to imperfect initial conditions.

1. Introduction

Accurate model predictions of mixed layer depth and temperature do not depend solely upon the model formulation. Ocean prediction is an initial boundary value problem that is highly dependent on the availability of oceanic observations. Furthermore, the upper ocean thermal and momentum structure prediction is also dependent on accuracy of the atmospheric forcing. Ocean prediction models require the fluxes of momentum and heat at the sea surface. A typical procedure is to use the bulk aerodynamic equations to specify sensible and latent heat fluxes, and to relate the short- and longwave radiation to the cloud cover. Consequently, the necessary atmospheric forcing variables include: wind speed, air temperature, dew point temperature, cloud amount and the sea surface temperature.

Errors in ocean prediction then fall into three categories: 1) those errors due to the physical limitations of the model, i.e., its simplifying assumptions and approximations; 2) errors due to imperfect initial conditions; and 3) errors due to uncertainty in the forcing. A technique known as data assimilation has recently been applied to study the errors in the second category. Elsberry and Warrenfeltz (1982) used data assimilation techniques to study the effect of erroneous temperature profiles on the prediction of mixed layer evolution at Ocean Weather Ship (OWS) Papa (50°N, 145°W). Larsen (1981) extended the Elsberry–Warrenfeltz study to include the effects of either incomplete or noisy verification temperature profiles, and the insertion of actual BT data taken at OWS Papa.

In this study, an approach similar to the data assimilation technique of Elsberry and Warrenfeltz (1982) is used to demonstrate the sensitivity of an ocean model to errors in the atmospheric forcing at Ocean Station Papa. Clancy (1979) investigated the effects of time-dependent forcing errors that increased linearly in time to simulate the uncertainty due to limited atmospheric model predictability. When the atmospheric error growth eliminated the upward heat flux at the surface, there were significant departures in only five days from the control run mixed layer depths and temperatures. In this study, errors are added to the actual observations to determine which atmospheric variables contribute most to upper ocean prediction model errors.

2. Method

Garwood and Adamec (1982) present a time series of atmospheric forcing and predicted mixed layer evolution at OWS Papa for 1953–69. In that study, the numerical representation is the oceanic planetary boundary layer (OPBL) prediction model of Garwood

(1977). The vertically-integrated, second order closure bulk method of Garwood (1977) is also the OPBL prediction model used in this study. The time-dependent boundary conditions of the surface flux of buoyancy and the solar radiation are derived from the 3 h observations of cloud cover, wind speed, sea surface temperature, air temperature and dew point temperature. The surface fluxes are computed using the formulas given in Appendix A. Notice that the 3 h observed sea surface temperature is necessary to calculate the sensible and latent heat fluxes. No other oceanographic observations are used in the annual simulations, except idealized initial temperature and salinity profiles are specified on 1 January of each year (1953–69).

The forcing parameters, model predicted sea surface temperature and observed and predicted mixed layer depths for the year 1965 are shown in Fig. 1. Only one fourth of the observed mixed layer depths (0.2°C below surface temperature) from the BTs are plotted since the number of observations completely obscures the predicted depths. The annual signal in both mixed layer depth and temperature is clearly evident. During winter, the mixed layer is over 100 m deep with an associated temperature of 5°C. Near Julian Day 90, the predicted and observed mixed layer suddenly retreats to a slightly shallower depth and undergoes another sudden retreat near Julian Day 135. The ability of the Garwood model to accurately and consistently predict deepening events and the times of retreat contributes to accurate prediction of the sea surface temperature. The trends in predicted and observed sea surface temperature are very similar, although the model predicts a slightly warmer mixed layer for most of the integration. There are other models which could have been used for this study, but the Garwood model has been extensively tested at Ocean Station Papa and has been shown to give reliable results for 17 separate years of integration (Garwood and Adamec, 1982).

Two "data windows" are chosen for this study: one representative of the winter regime (Julian days 50–65) and the other representative of summer conditions (Julian days 190–205). Hourly predictions of mixed layer temperature and depth from each season in each annual run are taken to be the control. The advantage of using model-generated temperatures and mixed layer depth is that a regular and complete set of "error-free" verification profiles is available. The disadvantage is that the model profiles do not contain all of the natural variability associated with advective and tidal processes that are omitted in this model. Because the same model is used in the sensitivity tests described below, only the relative error magnitudes between tests are meaningful.

The procedure is to rerun the ocean model with imperfect atmospheric forcing and determine the changes relative to the control run. The model is restarted at the beginning of each data window with the initial profile obtained from the control run, so that the model is initially "perfect." Separate integrations over the 15-day data window are then made while varying the atmospheric variables or the sea surface temperatures that are used to calculate the boundary conditions every 3 h. The magnitudes of the errors introduced in the forcing are based on a 17-year average of the standard deviation of that variable for that season. A listing of these standard deviations for the summer and winter regimes is given in Table 1. The assumption that the Gaussian error has a distribution proportional to the observed standard deviation of the variable is reasonable to establish an upper-bound on the expected observational errors. For detailed intercomparisons, one would have to choose appropriate proportionality constants for each variable. For example, one might expect that the forcing provided by an atmospheric prediction model would have proportionately larger errors in moisture or cloud cover than for air temperature.

Three sets of experiments are presented. Random errors with a Gaussian distribution are added to the atmospheric forcing variable in each case. The mean of the Gaussian error is adjusted to also permit negative or positive biases. Thus, the average error is either plus or minus $(1 - 1/e)$ times the magnitude of the 17-year standard deviation in Table 1, or is zero in the case of purely random errors. These three cases will be referred to as the "positive bias," "negative bias," and "random error" case studies, respectively. A normalized profile of the random error, positive and negative bias used for this study is given in Fig. 2. Some limits must be put on the modified variables. At no time is the wind speed or the cloud cover allowed to be negative. Also, the maximum cloud cover is not allowed to exceed unity.

3. Results

Some features of bulk mixed layer models that will assist in the first-order interpretation of the results are first reviewed. The mixed layer depth is governed approximately by

$$\Lambda \frac{\partial h}{\partial t} = \left(m_1 \frac{u_*^3}{h} - m_2 \alpha g \frac{Q_n}{\rho_0 C_p}\right) \Big/ (\alpha g \Delta T), \qquad (1)$$

where Q_n represents the total surface heat flux. The remainder of the symbols have their common meaning as given in Appendix B. When the prediction model is not in an entraining mode, the Heaviside step function is set equal to zero. In these situations, a new mixed layer depth can be derived from (1) by setting the right side equal to zero and obtaining

$$h = \frac{m_1 \rho_0 C_p u_*^3}{m_2 Q_n \alpha g}. \qquad (2)$$

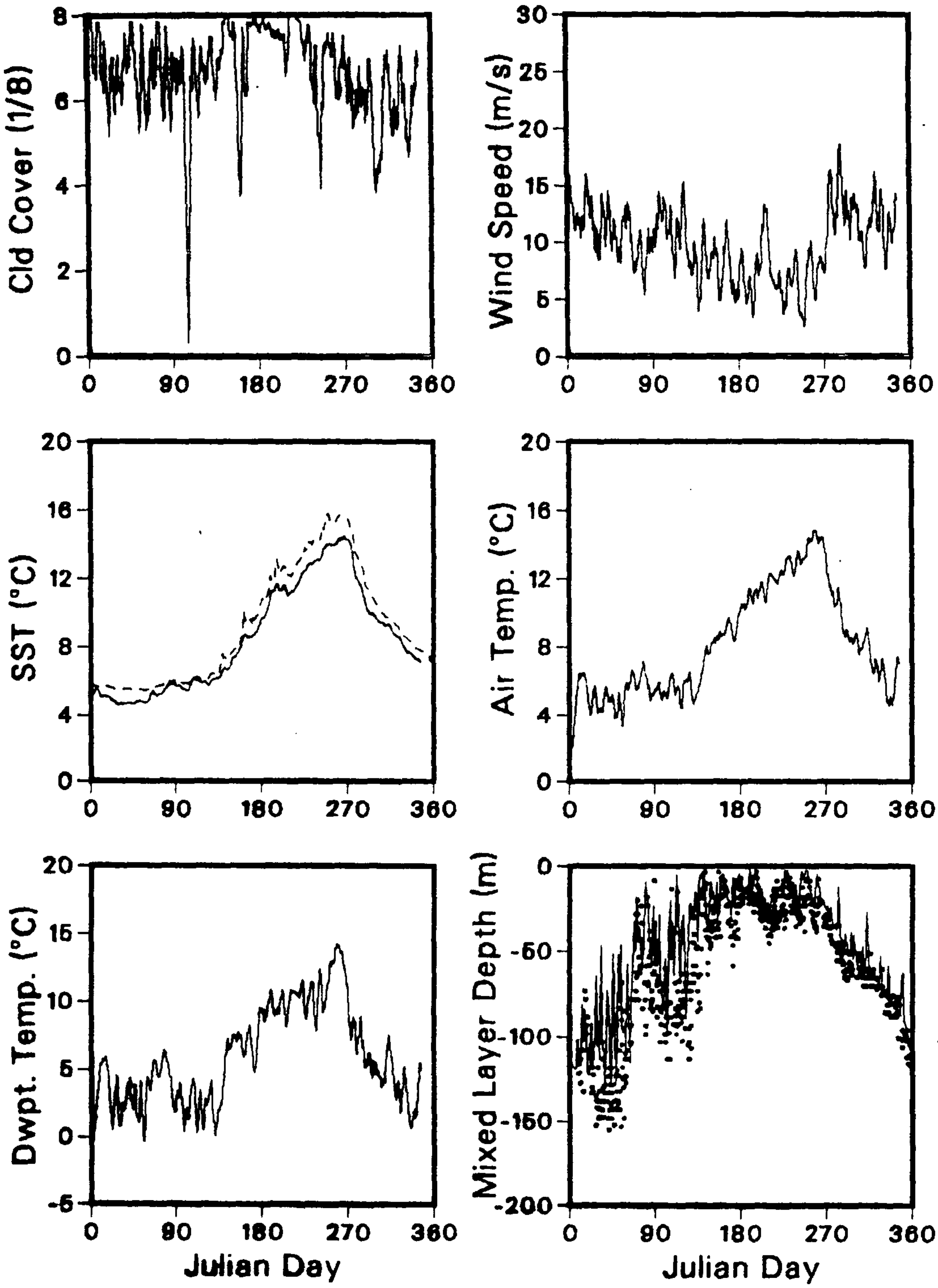

FIG. 1. Cloud cover, wind speed, observed and predicted (dashed line) sea surface temperature, air temperature, dew point temperature and observed and predicted (dots) mixed layer depths at OWS Papa during 1965.

It is expected that an error in the wind speed would be very detrimental in the prediction of the mixed layer depth because the wind speed enters as a cubic in (1) and (2), and also affects the sensible and evaporative heat fluxes (see formulas in Appendix A). Errors in the cloud cover would also be expected to be important since it is raised to the third power in the most important heating term (solar radiation) and to the

TABLE 1. Standard deviation (σ) of atmospheric variables and sea surface temperature observed at OWS Papa for winter and summer windows during 1953–69.

	σ	
	Winter	Summer
Cloud cover (eighths)	2.0	1.0
Wind speed (m s^{-1})	5.31	3.22
Sea surface temperature (°C)	0.24	0.50
Air temperature (°C)	1.21	0.81
Dew point temperature (°C)	2.44	1.19

second power in the back radiation. The dew point temperature is important in the calculation of the evaporative heat fluxes and also enters in the outgoing radiative heat flux. The air and sea surface temperatures both enter linearly in the calculation of the sensible heat flux and are not expected to be as important as the other parameters.

The year 1965 was selected for discussion because the ocean and atmospheric conditions are climatologically similar to most other years at Papa and also because the model exhibited a strong response to errors in the atmospheric forcing. During the winter window, the observed mixed layer depth varies between 100 and 150 m. The air, sea surface and dew point temperatures all fluctuate near their minimum values of 2–6°C, 3°C and 0–5°C respectively. The sea surface temperature does not exhibit much variability on the time scales shorter than the length of the data window (15 days). The wind speed averages about 12 m s^{-1} with high variability, and the cloud cover is consistently near $\frac{6}{8}$ or $\frac{7}{8}$. During the summer window, the mixed layer depth is usually between 5 and 20 m. The temperatures have not yet reached their maxima, but are all near 8 or 9°C. The wind speeds have diminished to about 7 m s^{-1} and there is typically completely overcast cloud conditions.

The results of the sensitivity studies that varied the cloud cover, wind speed and dew point temperature are shown for the winter and summer windows in Figs. 3a–f and 4a–f, respectively. The cases varying the air and sea surface temperatures are not shown since the response was not as dramatic. This is due to fairly uniform sea surface and air temperatures throughout these periods, so that magnitude of the errors that are being added or subtracted for these tests are relatively small. In Figs. 3 and 4, the mixed layer depth is a negative quantity, and all results are presented as deviations from the control run.

The most striking features in Figs. 3 and 4 are the differences between winter and summer mixed layer temperature and depth evolutions. Notice that the scales differ for the summer and winter case. As expected, the mixed layer depth errors during winter are much larger than during summer, whereas the errors in the mixed layer temperature are much more pronounced during summer than during winter. The sensitivity of the model predictions to erroneous atmospheric forcing is a strong function of season.

The following general features are evident in Figs. 3 and 4. Random errors with a zero mean do not affect the solution nearly as much as if there is a bias in the forcing. This is particularly evident in either the underestimation or over-estimation of wind speed or cloud cover. Adding (subtracting) a cloud bias will decrease (increase) the amount of solar radiation received at the surface and lead to larger (smaller) mixed layer depths and lower (higher) mixed layer temperatures. A positive (negative) bias in the wind speed will deepen (shallow) the mixed layer, and result in an effective decrease (rise) in the mixed layer temperature. Systematically higher (lower) dew point temperatures will effectively reduce (increase) the upward heat flux from the ocean and result in a warmer (colder) mixed layer, and smaller (larger) mixed layer depths.

Another feature of Figs. 3 and 4 is the relative magnitudes of the mixed layer depth and temperature differences associated with the individual forcing parameters. Recall that the Gaussian error is proportional to the observed standard deviation of each variable. For these conditions, the relative errors in mixed layer depth during winter are much larger for wind speed errors than for the dew point temperature and cloud cover. The relative magnitudes of mixed layer depth errors during summer are also larger for the imposed wind speed errors than for the other errors. Considering both temperature and depth differences during summer, the model sensitivity to the imposed cloud cover errors is larger than for the dew point temperature

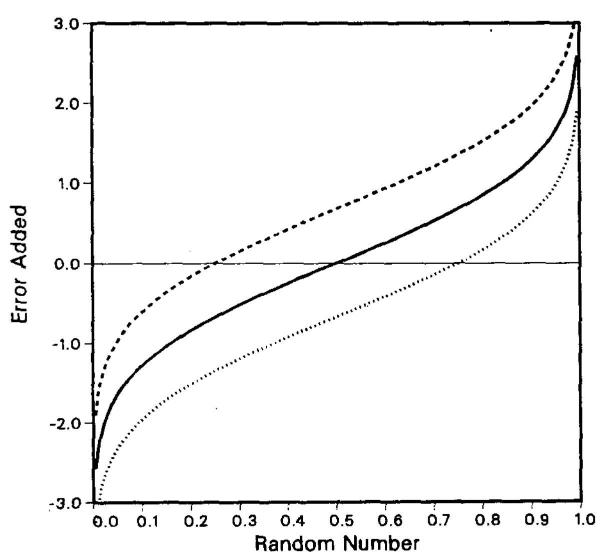

FIG. 2. Standard profile of errors added to the atmospheric forcing variables. The positive bias case is the dashed line, the negative bias case is the dotted line and the random error with zero mean is the solid line.

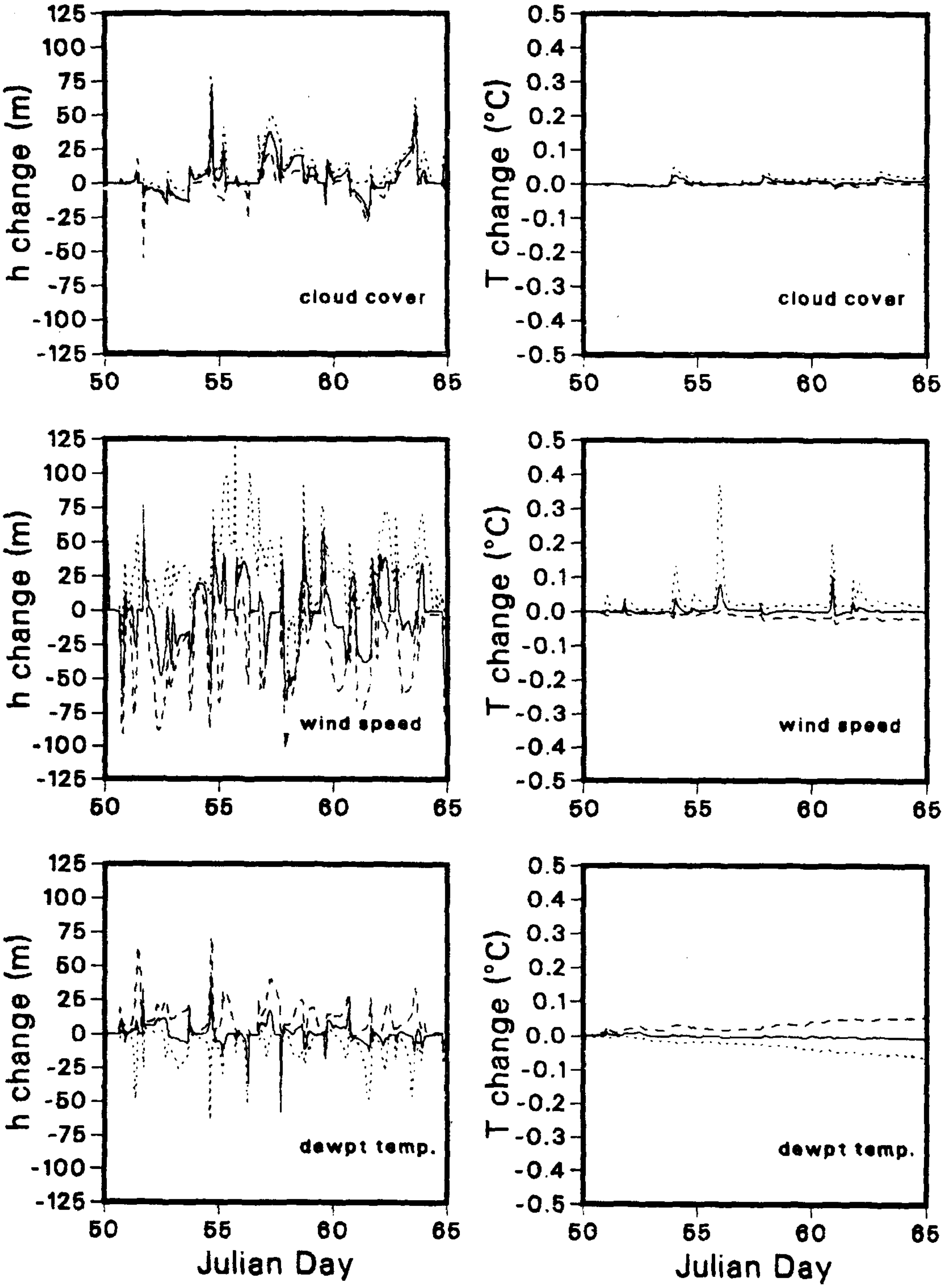

FIG. 3. Changes in well-mixed layer depth and temperature for winter 1965 varying cloud cover, wind speed and dew point temperature. The positive bias case is the dashed line, the negative bias case is the dotted line and the random error with zero mean is the solid line.

errors. These sensitivity tests give an indication of the relative errors that might be expected in the region of Ocean Station Papa from errors in the specification of atmospheric forcing.

For some forcing errors, the temperature differences grow steadily throughout the period, whereas the departures from the control appear more episodic for other forcing variables. An example of the nearly linear

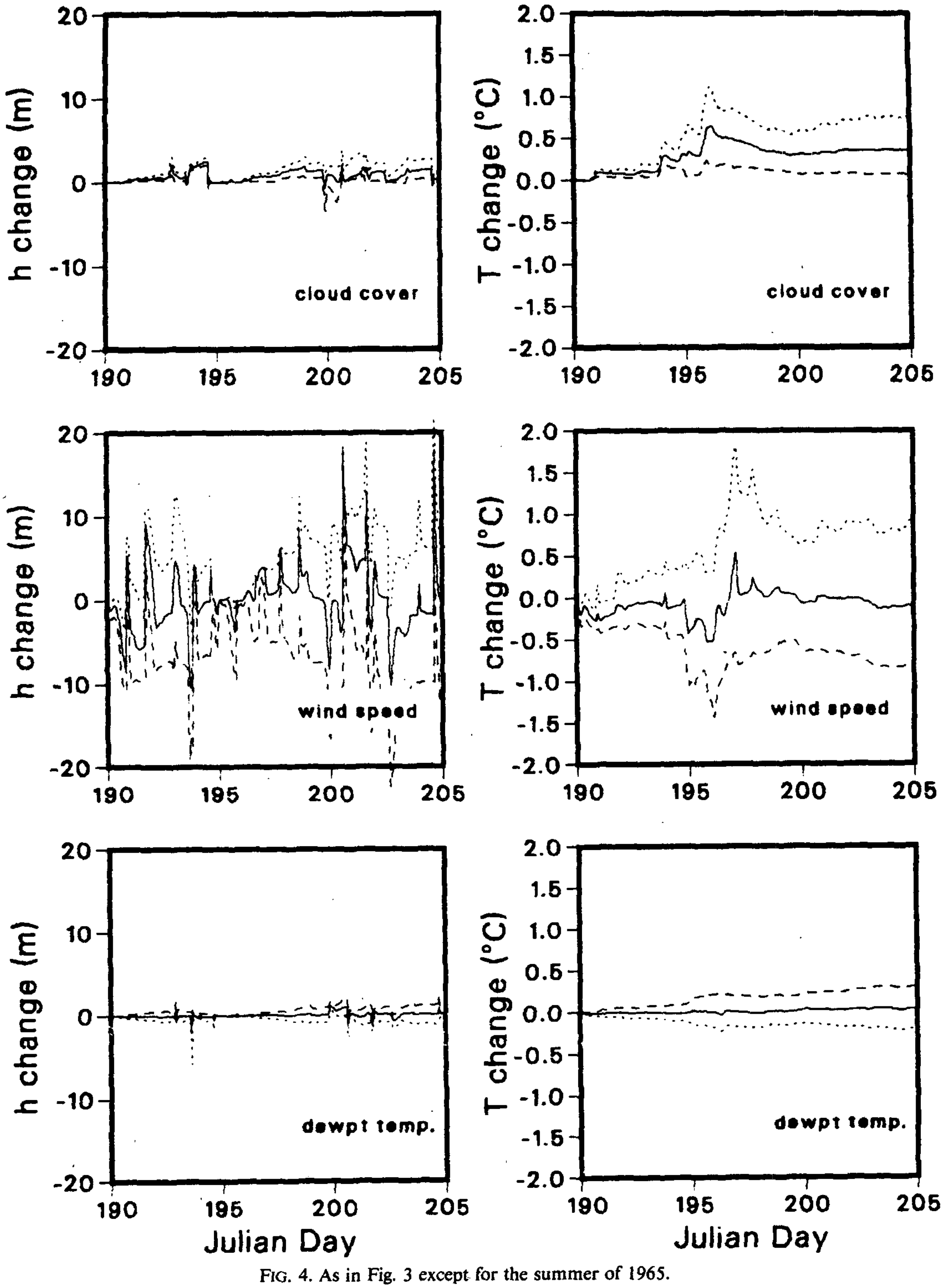

FIG. 4. As in Fig. 3 except for the summer of 1965.

growth is the response to dew point errors during winter (Fig. 3) or summer (Fig. 4). In the case of imposed wind speed errors, the temperature differences rise rapidly and then are more uniform in time. This behavior during winter is clearly related to the third power of the wind speed in (1) and the passage of strong forcing events. During summer the vertical redistribution of heat in the column is governed alternately by (1) during deepening events and by (2) during shallowing events. The energy input due to wind mixing is manifest as an increase in the potential energy of the upper layer. Wind mixing alone produces a larger density jump across the base of the mixed layer. Although a positive bias in the wind speed tends to set up a deeper mixed layer, the process is self-limiting due to the increase of stability below the mixed layer, which inhibits further entrainment. An analogous explanation applies in the negative bias case. By contrast, a change in the heat flux is stored directly in the mixed layer as a change in heat content. For example, the effect of surface cooling is to constantly erode the buoyancy jump. Hence, errors due to changes in the specification of heat flux will tend to accumulate with time.

A rms error and average absolute error are calculated at hourly intervals over the 15 days for each year. Because of the large number of cases, and because a rms or absolute error for each year rarely varied by more than 20%, an average of the 17 years of rms errors and absolute errors is given in Table 2 and 3. During winter, changes in wind speed produce rms errors in the mixed layer depth of over 25 m for both the positive bias and the negative bias case. Changes in dew point temperature, cloud cover, air temperature and sea surface temperature produce the next largest errors, respectively. During summer when sensitivity is more likely to appear in the temperature predictions, the changes in wind speed again produce the largest errors. The model sensitivity to a one standard deviation Gaussian error in the other forcing variables is not as large. The average absolute error is consistently near zero for any of the forcing variables for a random error with a zero mean. The positive bias and negative bias cases have nonzero mean errors of approximately the same magnitude, but of opposite signs. An exception to this systematic behavior is the case varying the cloud cover during summer. Garwood and Adamec (1982) showed that this midsummer period had a maximum of cloud cover, frequently with values of 1.0. Since cloud cover must always be less than, or equal to, 1.0, the addition of a positive bias had little effect.

TABLE 2. Root-mean-square and mean errors induced by deviations in the atmospheric forcing variables and sea surface temperature for the winter of years 1953–69. The depth errors are in meters and the temperature errors are in degrees Celsius.

	rms *H*	rms *T*	Error *H*	Error *T*
	Positive bias			
Cloud	7.69	0.01	−0.78	−0.00
Wind speed	38.87	0.04	−23.42	−0.03
SST	3.62	0.01	−1.67	−0.01
Air temperature	8.12	0.03	4.11	0.02
Dew point temperature	15.42	0.05	8.93	0.05
	Random error with zero mean			
Cloud	8.43	0.01	2.51	0.01
Wind speed	27.18	0.02	−2.25	−0.00
SST	2.01	0.00	−0.09	0.00
Air temperature	4.85	0.00	0.03	0.00
Dew point temperature	7.99	0.01	1.09	0.00
	Negative bias			
Cloud	11.46	0.02	5.71	0.01
Wind speed	36.75	0.06	22.78	0.03
SST	3.40	0.01	1.50	0.01
Air temperature	8.61	0.02	−4.01	−0.02
Dew point temperature	12.41	0.04	−6.05	−0.03

TABLE 3. As in Table 2 except for the summer

	rms *H*	rms *T*	Error *H*	Error *T*
	Positive bias			
Cloud	0.80	0.07	−0.06	−0.02
Wind speed	9.40	0.76	−7.42	−0.68
SST	0.61	0.13	−0.44	−0.11
Air temperature	0.41	0.09	0.30	0.08
Dew point temperature	0.86	0.20	0.64	0.18
	Random error with zero mean			
Cloud	1.19	0.21	0.69	0.18
Wind speed	4.40	0.24	−0.61	−0.16
SST	0.29	0.02	0.00	0.00
Air temperature	0.18	0.01	−0.00	0.00
Dew point temperature	0.40	0.03	0.04	0.01
	Negative bias			
Cloud	2.03	0.52	1.54	0.44
Wind speed	6.33	0.56	4.77	0.48
SST	0.61	0.13	0.44	0.12
Air temperature	0.41	0.09	−0.30	−0.08
Dew point temperature	0.78	0.16	−0.54	−0.14

4. Effects of forcing error amplitude

These tests of mixed layer model sensitivity to the atmospheric variables are somewhat qualitative because a specific error from Table 1 is applied. For completeness, one would also like a quantitative estimate of the mixed layer model accuracy for a range of uncertainties in the atmospheric forcing. The same tests are repeated with the magnitude of the standard deviation given in Table 1 multiplied by an "error factor" of 0.5, 1.5 and 2. Since the difference between model runs appeared primarily in errors in the winter mixed layer depth and the summer mixed layer temperatures, only the 17-year average of the cumulative 15-day errors is presented in Figs. 5 and 6.

As is the case of an individual year (Figs. 3 and 4) changes in the wind speed affect the predictions of mixed layer depth and temperature more than changes in any other variable. The average mixed-layer depth errors exceed 30 m with rms errors over 50 m, when the wind speed standard error is multiplied by a factor of 2. The corresponding mixed layer temperature errors are 0.5°C for the random error and negative bias case,

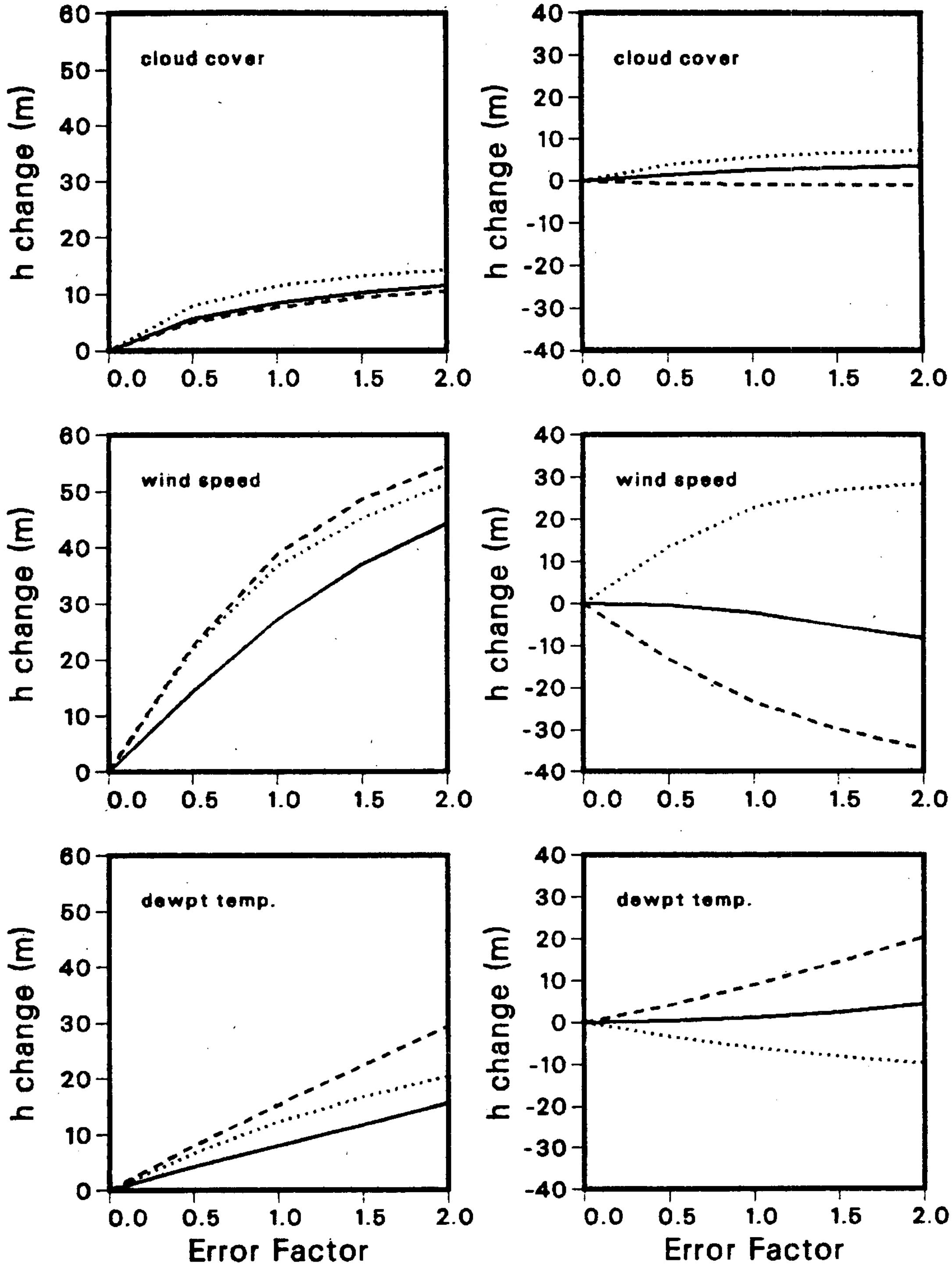

FIG. 5. Seventeen-year average of rms and mean mixed layer depth errors due to errors in cloud cover, wind speed and dew point temperature. The positive bias case is the dashed line, the negative bias case is the dotted line and the random error with zero mean is the solid line.

but near 1.5°C for the positive bias case. Errors associated with the air, sea surface and dew point temperature variations generally are less than 0.5°C, even when the error factor is 2. Average mixed layer depth variations of 15 m are also evident in winter when large dew point temperature errors are introduced and the corresponding rms errors are well over 30 m. Cloud cover, air and sea surface temperature changes pro-

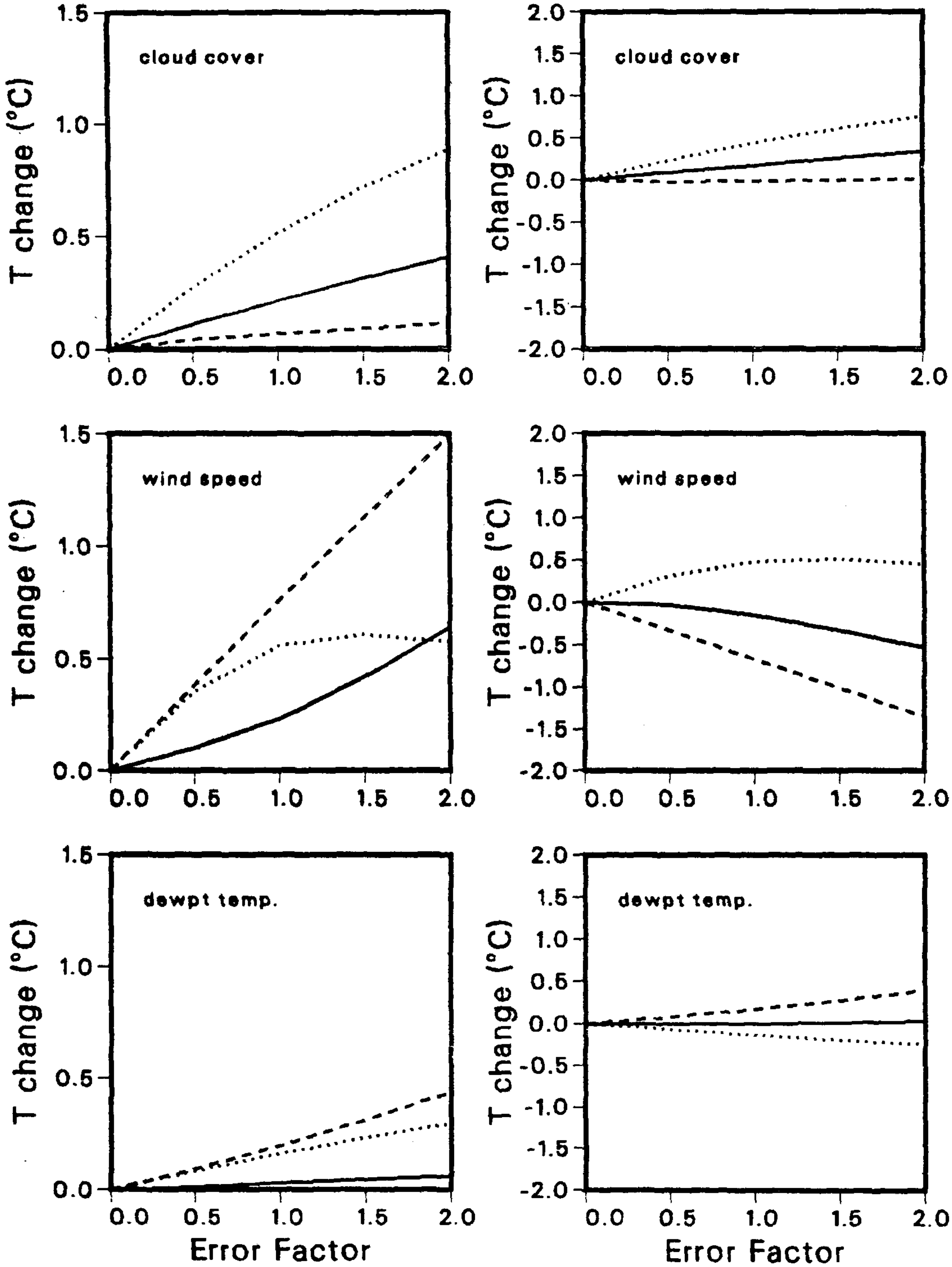

FIG. 6. As in Fig. 5 except for mixed layer temperature errors for summer.

duced average deviations of less than 10 m during winter.

An important point needs to be made for each of the variables in each of the test cases. There are no distinct changes in slope of the average deviations when plotted against uncertainty in the forcing. Indeed, except for the wind error effect on the winter mixed layer depth, the relationships are nearly linear. There is no obvious cutoff point. Finally, notice that if the random errors have a zero mean, there is little bias in the average mixed layer depth or temperature predictions. Although such a random error in the forcing may result in a temporary error in the ocean prediction, one might expect some cancelling of the error tendencies over model integrations of the length of these tests.

Because of the important role of atmospheric forcing for both OPBL and general circulation models, sensitivity studies can provide useful information on the effects of random errors in the input data on a model's predictive capability. Over data-sparse areas away from weather ships and merchant ship tracks, the atmospheric forcing will have to be provided by remote sensing techniques. Within the limitations of the mixed layer model used in this study, it appears that accuracy requirements for these atmospheric forcing estimates are quite stringent. These tests also indicate the relative accuracy that is required for each of the atmospheric forcing variables in ocean prediction. Given an acceptable error in either the mixed layer depth or temperature, one can quantitatively estimate the necessary accuracy in the atmospheric forcing variable. For example, to maintain the summer sea surface temperature predictions accurate to within 0.25°C, it is necessary to have an unbiased wind measurement to within 3.2 m s^{-1}.

It is also instructive to compare the magnitude of the prediction errors due to errors in the forcing to those due to uncertainty in the initial profile as in Elsberry and Warrenfeltz (1982). The Elsberry and Warrenfeltz (EW) study was repeated to include biases as well as random errors in the initial profile temperatures, mixed layer depths and thermocline slope. In addition, an error factor similar to above was used to illustrate the effect of varying ranges of observational errors in the temperature profiles.

The results for the winter mixed layer depth errors and summer mixed layer temperature errors are shown in Figs. 7 and 8. The effects of errors and biases introduced into the initial profile have far less of an

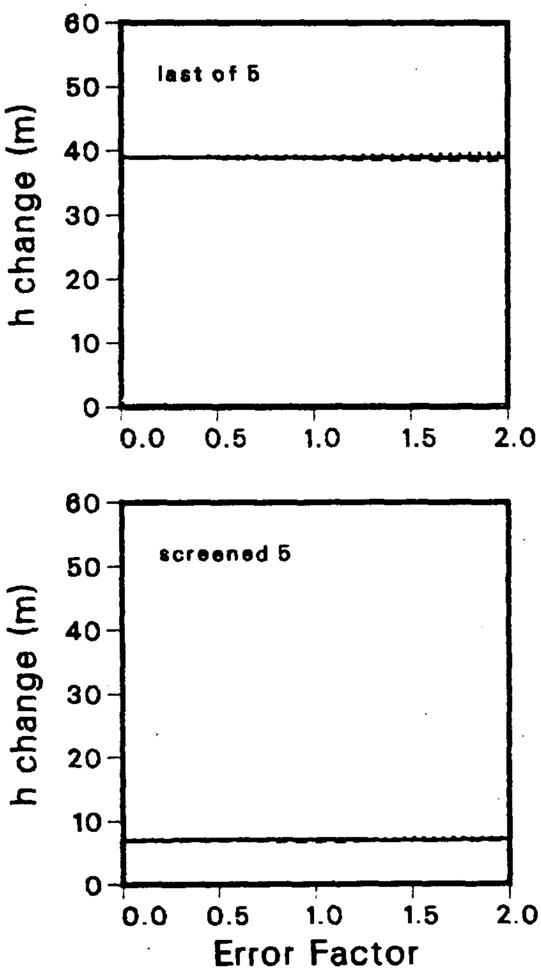

FIG. 7. Seventeen-year average of rms errors in winter mixed layer depth due to errors in the initial profile obtained by a last of 5 available profiles, an average of 5 profiles and a screen-average of 5 profiles. The positive bias case is the dashed line, the negative bias case is the dotted line and the random error with zero mean is the solid line.

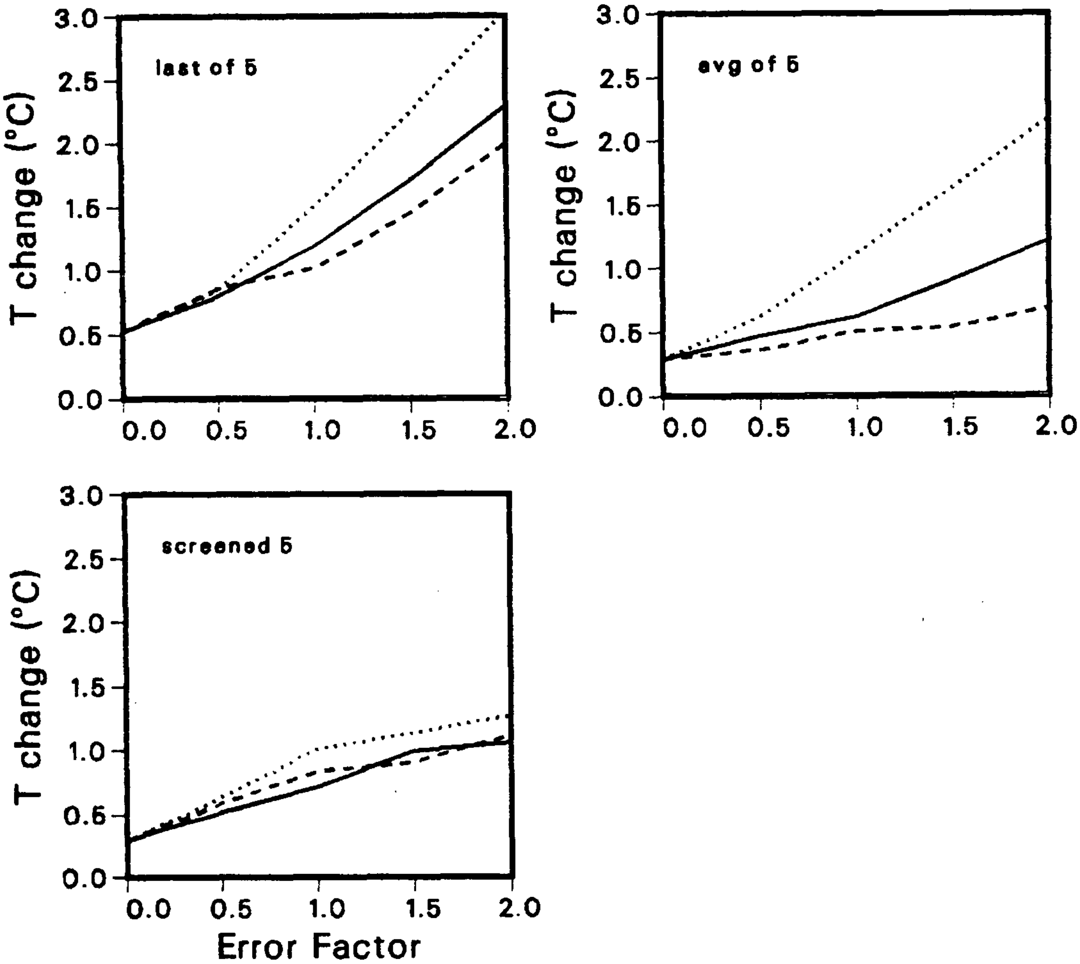

FIG. 8. As in Fig. 7 except for mixed layer temperature in the summer.

impact on the mixed layer depth predictions than do the differences between the assimilation methods used in EW to derive the initial profile. Most of the error in all of the methods displayed in Fig. 7 is evident even when the observational error is zero. The effect of an additional random error in the initial temperature profile is relatively small by comparison. As was the case in the original EW study, using an assimilation technique to obtain initial profiles is likely to produce a much more reliable prediction for the mixed layer depth than would occur if the last available profile was used. For these studies, the differences between the two methods of specifying the initial profile are 40 versus 8 m for the winter mixed layer depth and 0.3 versus 0.6°C for the summer mixed layer temperature.

5. Summary and conclusions

The results of including an error in the atmospheric forcing input to an OPBL model can be summarized as follows. First, the OPBL model is more sensitive to atmospheric forcing in the mixed layer depth predictions in the winter than in the summer. The errors are consistent with the observed natural variability in the ocean. That is, during winter when the mixed layer is deep and the temperatures are low, the errors in mixed layer depth predictions due to uncertainties in the atmospheric forcing are relatively large, and the errors in mixed layer temperature predictions are relatively small. Conversely, during summer errors in the mixed layer depth predictions become relatively small, and the errors in the mixed layer temperature predictions are relatively large. During winter or summer, the model predictions of mixed layer depth or temperature are most sensitive to a one standard deviation Gaussian error distribution in the wind speed.

The amount of error that is introduced in a prediction is necessarily a function of the uncertainty in the atmospheric forcing. This error growth rate is demonstrated by systematically increasing the errors associated with each variable in the atmospheric forcing. Bias, whether positive or negative, in the variable is more detrimental to the prediction than is a random error of large magnitude with zero mean. The effect of imperfect initial profiles produces forecast errors in the mixed layer depth and temperature comparable to those errors produced by uncertainties in the atmospheric forcing.

More studies of this type need to be done with other models of the upper ocean to assess confidently ocean predictability. The dramatic mixed layer shallowing during spring is likely to be very sensitive to atmospheric forcing (Elsberry and Garwood, 1978). The sensitivity of an ocean thermal prediction model to atmospheric forcing is very important since the date of spring transition will generally determine the character of the mixed layer variables for the entire summer. Not as dramatic, but certainly as important, changes occur during fall as the mixed layer gradually returns to a winter-type regime. Different locations in the ocean are also likely to show varying sensitivity to atmospheric forcing. It would also be useful to study the sensitivity of the entire upper ocean thermal structure to atmospheric forcing. Clancy (1979) indicates that the errors tend to accumulate at the base of the mixed layer, and thus may affect the temperature gradients at the top of the thermocline. Finally, similar studies could be done over a large area using a model capable of handling both advective and mixing effects.

Acknowledgments. The authors would like to thank Bob Haney for his helpful suggestions and comments regarding this manuscript. This research was sponsored by the Office of Naval Research under Contract NR 083-275 program element 61153N. All computations were performed at the W.R. Church Computer Center at the Naval Postgraduate School, Monterey, CA.

APPENDIX A

Formulas

Formulas used to calculate the atmospheric forcing for the Garwood (1977) mixed layer model; symbols are defined in Appendix B.

$$\left.\begin{aligned} u_*^2 &= \rho C_D|u|^2 \\ Q_E &= \rho C_E(q_s - q)|u| \\ Q_H &= \rho C_S(T_0 - T_A)|u| \\ Q_S &= S_0(1 - k_1C^3) \\ Q_B &= \sigma T_\theta(k_2 - q^{1/2})(1 - k_3C^2) \end{aligned}\right\} .$$

APPENDIX B

List of Symbols

C	cloud cover in eigths
C_D, C_E, C_S	drag coefficients for momentum, latent and sensible fluxes (1.3×10^{-3}, 1.42×10^{-3}, 1.5×10^{-3})
C_P	specific heat of water
g	acceleration due to gravity
h	mixed layer depth
k_1, k_2, k_3	constants related to absorption of radiation due to water vapor (1.105×10^{-3}, 7.8, 9.375×10^{-3})
m_1, m_2	mixing calibration constants (2.5, 1.0)
q, q_s	absolute humidity and saturated absolute humidity
Q_E, Q_H, Q_S, Q_B	latent, sensible, short-wave and back radiative heat fluxes
T_0, T_A	ocean and air temperatures
T, T_θ	ocean temperature and ocean temperature in absolute scale
S	incoming solar radiation at the top of the atmosphere
u, u_*	wind speed and friction velocity
α	coefficient of thermal expansion
Λ	Heaviside step function
ρ, ρ_0	density of air and seawater
σ	Stefan-Boltzman constant.

REFERENCES

Clancy, R. M., 1979: The effect of inaccuracies in meteorological parameters on one-dimensional forecasts of upper ocean thermal structure, SAI Rep. SAI-79-880-WA, 60 pp. [Available from Naval Ocean Research and Development Activity, NSTL Station, MS.]

Elsberry, R. L., and R. W. Garwood Jr., 1978: Sea-surface temperature anomaly generation in relation to atmospheric storms. *Bull. Amer. Meteor. Soc.*, **59**, 786–789.

——, and L. L. Warrenfeltz, 1982: Data assimilation test with an oceanic mixed layer model. *J. Phys. Oceanogr.*, **12**, 839–850.

Garwood, R. W., Jr., 1977: An oceanic mixed layer model capable of simulating cyclic states. *J. Phys. Oceanogr.*, **7**, 455–468.

——, and D. Adamec, 1982: Seventeen years of ocean mixed layer simulations at ocean station Papa, NPS Tech. Rep., ADA123732, 37 pp.

Larsen, D. G., 1981: Oceanic data assimilation tests with a one-dimensional model, M.S. thesis, NTISA115175, Naval Postgraduate School, Monterey, CA, 71 pp.